Fractional chiral superconductors

Eran Sagi,[1] Arbel Haim,[1] Erez Berg,[2] Felix von Oppen,[3] and Yuval Oreg[1]

[1]*Department of Condensed Matter Physics, Weizmann Institute of Science, Rehovot, Israel 76100*
[2]*Department of Physics, University of Chicago, Chicago, Illinois 60637, USA*
[3]*Dahlem Center for Complex Quantum Systems and Fachbereich Physik, Freie Universitat Berlin, 14195 Berlin, Germany*

Two-dimensional $p_x + ip_y$ topological superconductors host gapless Majorana edge modes, as well as Majorana bound states at the core of $h/2e$ vortices. Here we establish the possibility of realizing the fractional counterpart of this phase: a fractional chiral superconductor. This exotic phase is shown to give rise to a plethora of non-Abelian bulk excitations and a chiral $\mathbb{Z}_{2m}$ parafermion theory on the edge of the sample, where m is an odd integer. In addition, we demonstrate that $\mathbb{Z}_{2m}$ parafermionic bound states reside at the cores of $h/2e$ vortices. In certain geometries, the system can support a fractional Josephson junction with $4\pi m$ periodicity, reflecting the underlying non-Abelian excitations. Finally, we show that the tunneling density of states associated with this edge theory exhibits an anomalous energy dependence of the form ω^{m-1}. Our results are demonstrated through an explicit tractable model, composed of an array of coupled Rashba wires in the presence of strong interactions, Zeeman field, and proximity coupling to an s-wave superconductor.

I. INTRODUCTION

Much is known nowadays about topological states in quadratic fermion systems. In such cases, the topological states protected by time-reversal, particle-hole, and chiral symmetries have been classified [1,2]. Beyond this celebrated periodic table, topological phases protected by other symmetries such as lattice symmetries [3–13] have also been thoroughly studied.

In contrast, strongly interacting topologically ordered phases which cannot be realized in the absence of interactions have yet to be fully understood and classified. Since interactions stabilize these phases, their study generally requires nonperturbative methods. In this work, we propose strongly interacting superconducting phases that are natural fractional counterparts of the noninteracting $p_x + ip_y$ chiral superconductor: *fractional* chiral superconductors (FCSCs).

A noninteracting $p_x + ip_y$ superconductor hosts a chiral Majorana mode or, equivalently, a $\mathbb{Z}_2$ parafermion theory, at the edge. In contrast, the edge of the FCSC phases we find is described by nontrivial $\mathbb{Z}_{2m}$ parafermion conformal field theories (CFTs), where m can be any odd integer. This makes the FCSC phases close relatives of the well-known $\mathbb{Z}_{2m}$ Read-Rezayi quantum Hall states [14], whose edge theories have identical non-Abelian components. In addition, while an $h/2e$ vortex in a $p_x + ip_y$ superconductor binds a Majorana zero mode, a vortex in the FCSC phases binds $\mathbb{Z}_{2m}$ parafermion zero modes. Unlike the $p_x + ip_y$ superconductor, however, an FCSC phase generally contains a rich set of deconfined non-Abelian excitations even in the absence of vortices.

Remarkably, we present an analytically tractable model realizing these strongly interacting phases. This allows us to explicitly study their properties and experimental signatures in detail. The model consists of an array of wires with Rashba spin-orbit coupling in the presence of a Zeeman field and proximity coupling to an s-wave superconductor [see Fig. 1(a)]. For this system, it is useful to define a "filling factor" ν as the number of electrons in a spin-orbit length [see Eq. (2)]. It was previously shown that a $p_x + ip_y$ superconductor phase arises at filling $\nu = 1$ [15]. In the

presence of strong interactions, we show that FCSC phases can emerge at fractional filling factors of the form $\nu = 1/m$ for m odd.

We analyze the model by mapping the low-energy theory of the individual wires to a generalized Sine-Gordon model. Performing an ϵ expansion for $m = 2 + \epsilon$, we show that each wire can be tuned to a $\mathbb{Z}_{2m}$ parafermion multicritical point [16]. We then demonstrate that one can couple different wires in such a way that all the bulk modes get gapped and a chiral $\mathbb{Z}_{2m}$ parafermion CFT is left on the edge. By construction, the resulting two-dimensional (2D) model is topologically ordered for $m > 1$.

By considering a Corbino geometry [see Fig. 3(a)], we are able to study $h/2e$ vortices in the system. We show that these vortices host non-Abelian parafermion zero modes by mapping our configuration to domain walls on the edge of a 2D fractional topological insulator (TI) [17–19].

As a possible experimental signature of the predicted phase, we examine the Josephson junction depicted in Fig. 1(b), in which the superconductor stabilizing the FCSC is cut into two concentric annuli. In the quasi-one-dimensional (thin annulus) regime, where coupling between the two edges is allowed, the radial Josephson current is shown to exhibit a $4\pi m$ periodicity as a function of the superconducting phase difference.

The coupled-wires approach has been extensively used to describe different strongly interacting topological phases [15,20–39]. In addition, fractional superconducting phases were previously discussed, mostly from a field-theoretic point of view, in Refs. [40–42]. However, a direct fractional analog of the $p_x + ip_y$ superconductor has not been found. The FCSC phase we propose is clearly distinct from previously discussed phases in its bulk and edge physics, and appears to constitute a natural fractional extension of the $p_x + ip_y$ superconductor.

The structure of the paper is as follows: In Sec. II, we describe our model and review the construction of a $p_x + ip_y$ superconductor described in Ref. [15]. In Sec. III, we study the model at fractional filling factors in the presence of strong interactions and demonstrate the emergence of FCSC phases.
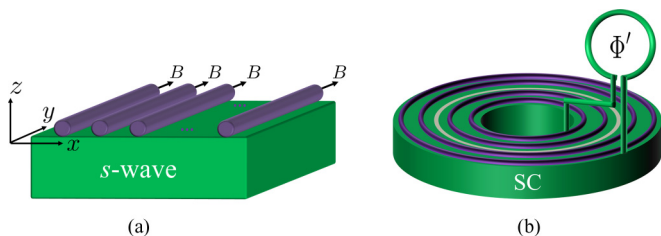
FIG. 1. (a) A schematic view of the system we use to construct a two-dimensional fractional chiral superconductor (FCSC). The system is composed of an array of N weakly coupled wires with strong Rashba spin-orbit coupling. We demonstrate that the interplay of the Zeeman field, proximity to an s-wave superconductor, and strong interactions can result in an FCSC phase with a chiral parafermion CFT at the edges of the sample and parafermionic bound states at the core of vortices. (b) A Corbino geometry, used in order to study $h/2e$ vortices and the anomalous Josephson effect. By connecting the internal and external parts with a superconducting wire, through which flux can be inserted, the relative phases between the two superconducting regions can be controlled. It is argued that in the quasi-one-dimensional regime, this configuration is equivalent to the effective junction shown in Fig. 3(f), leading to a $4\pi m$-periodic Josephson effect.

In Sec. IV, we study the non-Abelian defects associated with $h/2e$ vortices and their imprints through the Josephson effect.

II. TOPOLOGICAL SUPERCONDUCTOR FROM AN ARRAY OF COUPLED WIRES

We start by reviewing the construction of a $p_x + ip_y$ superconductor, presented in Ref. [15]. In Sec. III, the construction of the fractional phases will proceed in parallel to that of the $p_x + ip_y$ phase, replacing the electron operators in the noninteracting case with new local fermionic operators composed of an electron dressed by particle-hole excitations. These new degrees freedom are similar to those that arise in the wire construction of the $\nu = 1/m$ fractional quantum Hall states [20].

The starting point is an array of decoupled Rashba wires. Similar to Refs. [43,44], each wire is subjected to a Zeeman field and proximity coupled to an s-wave superconductor,

$$H = \sum_n \int dx \, \vec{\psi}_n^\dagger(x) \left[-\frac{(\partial_x - iuM\sigma_z)^2}{2M} - \mu + B\sigma_x \right] \vec{\psi}_n(x)$$
$$+ \int dx [\Delta \psi_{n\uparrow}^\dagger(x) \psi_{n\downarrow}^\dagger(x) + \text{H.c.}]. \quad (1)$$

Here, $\vec{\psi}_n = [\psi_{n\uparrow}(x) \quad \psi_{n\downarrow}(x)]^T$, where $\psi_{ns}(x)$ represents the electron annihilation operator at wire number n with spin s [see Fig. 1(a)]. The matrices σ_i are Pauli matrices operating on the spin degrees of freedom. The parameters u, B, and Δ are the Rashba spin-orbit coupling (SOC), the Zeeman field, and the induced superconducting pairing potential, respectively.

Figure 2 presents the spectrum of a single wire in the absence of superconductivity and a Zeeman field ($B = \Delta = 0$). We define the Fermi momentum $k_F^0 = \sqrt{2M\mu}$ in the absence of SOC, and the shift $k_{so} = Mu$ of the parabolas due to SOC. In terms of these, the filling fraction of the system is
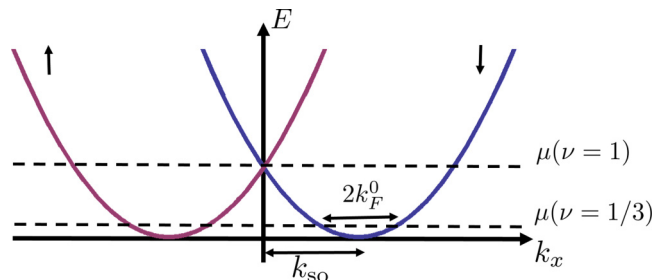

FIG. 2. The spectrum of an individual wire in the absence of interactions, Zeeman field, and proximity coupling. The dashed lines specify the chemical potentials corresponding to the situations $\nu = 1$ and $\nu = 1/3$.

defined as

$$\nu = k_F^0 / k_{so}. \quad (2)$$

To study the low-energy physics, we linearize the spectrum near the Fermi level and decompose the fermionic modes into right- and left-moving modes,

$$\psi_{ns}(x) = \psi_{nsR}(x) + \psi_{nsL}(x), \quad (3)$$

with $\psi_{ns\rho}(x) = \psi_{ns\rho}^0(x)e^{ik_{s\rho}x}$. Here, $\psi_{ns\rho}^0$ are the low-energy degrees of freedom near the Fermi momenta $k_{s\rho} = \rho k_F^0 - sk_{so}$ (where $\rho = \pm 1$ denotes a right-/left-moving mode).

The $p_x + ip_y$ superconductor corresponds to $\nu = 1$. Focusing on the low-energy excitations for $|\Delta - B| \ll B, \Delta$, the Zeeman term $H_B = \int dx [B\psi_{n\uparrow R}^\dagger(x)\psi_{n\downarrow L}(x) + \text{H.c.}]$ and the pairing term $H_\Delta = \int dx \{\Delta[\psi_{n\uparrow R}^\dagger(x)\psi_{n\downarrow L}^\dagger(x) + \psi_{n\uparrow L}^\dagger(x)\psi_{n\downarrow R}^\dagger(x)] + \text{H.c.}\}$ gap out the wires (see Fig. 2). Indeed, the second term in H_Δ fully gaps the high-momentum degrees of freedom $\psi_{n\uparrow L}$ and $\psi_{n\downarrow R}$, and the low-momentum degrees of freedom $\psi_{n\uparrow R}$ and $\psi_{n\downarrow L}$ are coupled by the Zeeman term H_B as well as the first term of H_Δ. The fully gapped phases for $\Delta > B$ and $\Delta < B$ are topologically distinct—the first is a 1D trivial phase, while the second is a topological superconductor. For $B = \Delta$, the intermode part of the Hamiltonian, given by $H_\Delta + H_B$, commutes with the operators

$$\alpha_n(x) = \psi_{n\uparrow R}(x) + \psi_{n\uparrow R}^\dagger(x),$$
$$\beta_n(x) = -i[\psi_{n\downarrow L}(x) - \psi_{n\downarrow L}^\dagger(x)], \quad (4)$$

so the system is gapless.

Tuning to this transition point, we introduce an interwire term of the form

$$H_\perp = it_\perp \sum_n \int dx \, \alpha_n(x) \beta_{n+1}(x). \quad (5)$$

This term arises naturally in the system of Fig. 1(a) due to a combination of interwire hopping, superconductivity, and spin-orbit interaction [15]. It gaps out the bulk degrees of freedom, yet it leaves the Majorana fields $\beta_1(x)$ and $\alpha_N(x)$ decoupled, thus stabilizing a $p_x + ip_y$ phase. This construction can be considered the anisotropic limit of the system studied by Refs. [45,46]. While it relies on a fine-tuned relation between parameters, the resulting phase is independent of

these assumptions, remaining qualitatively identical as long as the bulk gap remains open.

III. FRACTIONAL CHIRAL SUPERCONDUCTORS

To construct a FCSC phase at filling $\nu = 1/m$, we consider the effects of strong interactions within a bosonized description of the 1D degrees of freedom. Using the standard Abelian bosonization technique, we describe the Hilbert space in terms of bosonic fields $\phi_{ns\rho}$ via $\psi_{ns\rho} \propto e^{i(\phi_{ns\rho} + k_{s\rho}x)}$. The boson fields satisfy the commutation relations

$$[\phi_{ns\rho}(x), \phi_{n's'\rho'}(x')] = i\pi\rho\,\delta_{nn'}\delta_{ss'}\delta_{\rho\rho'}\,\mathrm{sgn}(x - x') + i\pi A^{n's'\rho'}_{ns\rho},$$
(6)

where $A^{n's'\rho'}_{ns\rho}$ takes the values ± 1 for any $\{ns\rho\} \neq \{n's'\rho'\}$ and is antisymmetric with respect to the exchange $\{ns\rho\} \leftrightarrow \{n's'\rho'\}$ (ensuring that the fermionic anticommutation relations are satisfied).

For $\nu = 1/m$, it is useful to define new chiral fermion operators $\tilde{\psi}_{ns\rho} = e^{i(\eta_{ns\rho} + q_{s\rho}x)}$, with

$$\eta_{ns\rho} = \frac{m+1}{2}\phi_{ns\rho} - \frac{m-1}{2}\phi_{ns\bar{\rho}}.$$
(7)

The new fields $\tilde{\psi}_{ns\rho}$ are fermionic, as evident from the commutation relations

$$[\eta_{ns\rho}(x), \eta_{n's'\rho'}(x')] = im\pi\rho\,\delta_{nn'}\delta_{ss'}\delta_{\rho\rho'}\,\mathrm{sgn}(x - x') + i\pi\tilde{A}^{n's'\rho'}_{ns\rho},$$
(8)

where $\tilde{A}^{n's'\rho'}_{ns\rho}$ takes odd integer values for any $\{ns\rho\} \neq \{n's'\rho'\}$ and is antisymmetric with respect to the exchange $\{ns\rho\} \leftrightarrow \{n's'\rho'\}$. The $\tilde{\psi}_{ns\rho}$ fields carry momenta $q_{s\rho} = \frac{m+1}{2}k_{s\rho} - \frac{m-1}{2}k_{s\bar{\rho}}$.

Note that the momenta $q_{s\rho}$ carried by the new fields $\tilde{\psi}_{ns\rho}$ match those of a $\nu = 1$ wire. In particular, the operators $\tilde{\psi}_{n\uparrow R}$ and $\tilde{\psi}_{n\downarrow L}$ now have vanishing oscillatory components, allowing us to couple them in various ways without breaking translational symmetry.

Once the Zeeman term is dressed by intrawire $2k_F$ interactions, it induces a term of the form $\tilde{H}_B = \int \frac{dx}{a^2}[\tilde{B}\,\tilde{\psi}^{\dagger}_{n\uparrow R}(x)\tilde{\psi}_{n\downarrow L}(x) + \text{H.c.}]$ (where a is the short distance cutoff). We assume that $\tilde{B}$ is large enough such that this term gaps out the small momentum fields $\tilde{\psi}_{n\uparrow R}$ and $\tilde{\psi}_{n\downarrow L}$. We may also write dressed pairing terms of the form $\tilde{H}_\Delta = \int \frac{dx}{a^2}\{\tilde{\Delta}[\tilde{\psi}^{\dagger}_{n\uparrow R}(x)\tilde{\psi}^{\dagger}_{n\downarrow L}(x) + \tilde{\psi}^{\dagger}_{n\uparrow L}(x)\tilde{\psi}^{\dagger}_{n\downarrow R}(x)] + \text{H.c.}\}$. As in the $\nu = 1$ case, the second term in $\tilde{H}_\Delta$ involves high-momentum degrees of freedom and does not compete with the Zeeman term, $\tilde{H}_B$. It fully gaps out the fields $\tilde{\psi}_{n\uparrow L}$ and $\tilde{\psi}_{n\downarrow R}$. The first term in $\tilde{H}_\Delta$ competes with the Zeeman field $\tilde{H}_B$. For $\tilde{\Delta} = \tilde{B} = \lambda$, one obtains a critical theory, similar to the $\nu = 1$ case, which in this case is described by a $\beta^2 = 4\pi m$ self-dual Sine-Gordon model (see Appendix A):

$$H = \int dx[(\partial_x\theta)^2 + (\partial_x\varphi)^2$$
$$\times \frac{\lambda}{a^2}\{\cos(\sqrt{4\pi m}\varphi) + \cos(\sqrt{4\pi m}\theta)\}],$$
(9)

where we have defined $\varphi = \frac{\eta_{n\uparrow R} - \eta_{n\downarrow L}}{2\sqrt{\pi m}}$ and $\theta = \frac{\eta_{n\uparrow R} + \eta_{n\downarrow L}}{2\sqrt{\pi m}}$.

It is, however, *a priori* unclear whether the critical line $\tilde{B} = \tilde{\Delta}$ is dominated by the $\tilde{B}$ and $\tilde{\Delta}$ terms. In the weak-coupling limit, both $\tilde{B}$ and $\tilde{\Delta}$ flow to zero, giving a trivial Luttinger-liquid fixed point. However, it turns out that when $\tilde{B}$ and $\tilde{\Delta}$ are equal and large enough, a nontrivial multicritical point is encountered.

To show this, we follow the analysis in Ref. [47] and employ an ϵ expansion, with $m = 2 + \epsilon$. In this approach, the scaling dimensions of the $\tilde{B}$ and $\tilde{\Delta}$ terms are small, thus pushing the competition between the first- and higher-order terms of the renormalization-group (RG) equations to the region in which the perturbative RG analysis applies. As we show in Appendix A, the RG equation describing the flow of $\lambda = \tilde{B} = \tilde{\Delta}$ takes the form

$$\frac{d\lambda}{dl} = -\epsilon\lambda + \pi^2\lambda^3.$$
(10)

When $\lambda > \sqrt{\epsilon}/\pi$, a flow to large coupling ensues and the low-energy theory is no longer capable of describing the model. The point $\lambda = \sqrt{\epsilon}/\pi$ is a multicritical point separating the $\tilde{B}$-dominated phase, the $\tilde{\Delta}$-dominated phase, and the gapless phase. Extrapolating to ϵ of the order of unity, we assume that such a critical point persists. For completeness, we study the full phase diagram of the system in Appendix A.

To uncover the nature of the CFT describing the multicritical point, it is useful to review the physics of classical 2D $\mathbb{Z}_k$ (clock or Potts) models. As discussed in detail in Refs. [48–50], such models possess self-dual lines. For $k \leqslant 4$, there is a self-dual critical point that separates the disordered and ordered ($\mathbb{Z}_k$ symmetry-broken) phases. For $k > 4$, some regions of the self-dual line are contained in gapless phases, while others consist of first-order transitions. The different regions of the self-dual line are separated by multicritical points [48,50]. It was argued in Ref. [16] that these are described by a $\mathbb{Z}_k$ parafermion CFT. In addition, it is well known that the low-energy physics of self-dual $\mathbb{Z}_k$ models is described by $\beta^2 = 2\pi k$ self-dual Sine-Gordon models [51,52]. The above prompts us to identify the finite-coupling multicritical point in our self-dual Sine-Gordon models with those of the $\mathbb{Z}_k$ models. This indicates that our model at the multicritical point is described by a $\mathbb{Z}_{2m}$ parafermion CFT.

In what follows, we assume that each wire is tuned to the multicritical point and is therefore described by a $\mathbb{Z}_{2m}$ parafermion theory. At this critical point, the fields

$$\tilde{\alpha}_n(x) = e^{i\eta_{n\uparrow R}(x)} + e^{-i\eta_{n\uparrow R}(x)},$$
$$\tilde{\beta}_n(x) = -i[e^{i\eta_{n\downarrow L}(x)} - e^{-i\eta_{n\downarrow L}(x)}]$$
(11)

commute with the intermode Hamiltonian $\tilde{H}_B + \tilde{H}_\Delta$. As we demonstrate in Appendix B, the propagators describing this low-energy theory take the form $\langle\tilde{\alpha}_n(z)\tilde{\alpha}_n(z')\rangle \propto (z - z')^{-m}$ and $\langle\tilde{\beta}_n(\bar{z})\tilde{\beta}_n(\bar{z}')\rangle \propto (\bar{z} - \bar{z}')^{-m}$, with $z = x + i\tau$. We identify these fields with the ψ_m and $\bar{\psi}_m$ primary fields of the $\mathbb{Z}_{2m}$ theory, which indeed have conformal dimension $m/2$ [16].

Similar to the noninteracting case [see Eq. (5)], we introduce the interwire term

$$\tilde{H}_\perp = i\tilde{t}_\perp \sum_n \int \frac{dx}{a^2}\tilde{\alpha}_n(x)\tilde{\beta}_{n+1}(x).$$
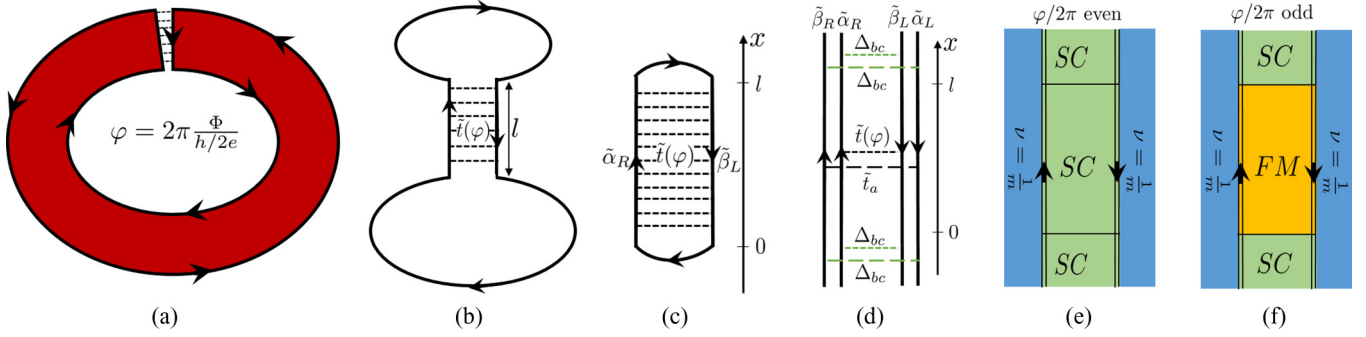(12)

FIG. 3. A schematic depiction of the line of arguments used in order to identify the zero modes localized at the center of $h/2e$ vortices. (a) We start by placing our FCSC phase in an annular geometry, through which a magnetic flux may be inserted. Without altering the essential characteristics of the system, we cut a thin trench through the annulus. (b) As the presence of zero modes should not depend on the precise geometry as long as the topological structure is preserved, we focus on the edge theory and fold our system inside out to a bone-shaped geometry. (c) The independence on the precise geometry allows us to shrink the outermost regions. (d) We examine an auxiliary model which has twice as many degrees of freedom, but whose low-energy sector coincides with our model. We then show that the auxiliary model in (d) can be adiabatically deformed into a system composed of $\nu = 1/m$ fractional quantum Hall edges coupled by ferromagnetic and superconducting terms. (e) If the flux φ is an even multiple of 2π, we get the effective superconducting term throughout the system, meaning there are no zero modes. (f) For odd multiples of 2π, the superconductor in the physical region is replaced by a ferromagnet. The domain walls of the resulting configuration, representing the edges of the original configurations, give rise to parafermionic bound states [17–19].

Since the interwire Hamiltonian in Eq. (12) has the same form as the self-dual intrawire Hamiltonian and is composed of fields which commute with the intrawire coupling terms, $\tilde{t}_\perp$ flows according to the RG equation (10). Therefore, if $\tilde{t}_\perp$ is large enough, a flow to large coupling ensues and this Hamiltonian leaves the fields $\tilde{\beta}_1$ and $\tilde{\alpha}_N$ gapless. These fields represent the local electron operators on the edges. In fact, a full chiral $\mathbb{Z}_{2m}$ parafermion CFT is expected to reside on each edge. Using the propagator of the $\tilde{\alpha}$ and $\tilde{\beta}$ fields, we find that the electrons' tunneling density of states $N(\omega)$, associated with the edge, scales with an anomalous exponent: $N(\omega) \propto \omega^{m-1}$.

Similar to the noninteracting case, the strict constraints on the various parameters may be lifted as long as the bulk gap does not close.

IV. NON-ABELIAN DEFECTS AND $4\pi m$-PERIODIC JOSEPHSON EFFECT

To study the non-Abelian defects residing at the core of vortices, we examine the configuration presented in Fig. 3(a). The FCSC is shaped like an annulus and the flux threading the annulus is given by an odd multiple of $h/2e$ [60]. In analogy to the noninteracting case [53], we expect to find zero modes on the two edges of the system. It will prove useful to cut a thin trench in the annulus. In this case, the flux through the center of the annulus can be chosen to enter in the coupling across the trench, and we can deform our system in such a way that connects it with the configuration studied in Refs. [17–19] [see Fig. 3(f)].

Given that we are only interested in finding zero-energy modes, we have a large amount of freedom in deforming the geometry of the problem while preserving its topology. We first fold the edge "inside out," leading to the bone-shaped configuration depicted in Fig. 3(b). We may then shrink the outermost regions without introducing interedge coupling. This leads to the simple 1D geometry presented in Fig. 3(c), in

which the counterpropagating edge modes $\tilde{\alpha}_R$ and $\tilde{\beta}_L$ (defined in the region $0 < x < l$) are connected at $x = 0, l$.

The zero-mode properties are solely encoded in the low-energy edge theory. We therefore have the additional freedom of changing the Hamiltonian governing the gapped degrees of freedom. One must only ensure that the modes $\tilde{\alpha}_R$ and $\tilde{\beta}_L$, and the other primary fields of the parafermion CFT, remain gapless, while the other microscopic degrees of freedom, such as $\tilde{\alpha}_L$ and $\tilde{\beta}_R$, remain gapped.

An auxiliary model, in which the latter fields are coupled directly while bulk degrees of freedom are projected out, satisfies this condition. The corresponding Hamiltonian is given by

$$
\begin{aligned}
H_{\text{auxiliary}} &= i\tilde{t}_a \int_0^l dx\, \tilde{\beta}_R(x)\tilde{\alpha}_L(x) \\
&= \tilde{t}_a \int_0^l dx\, [\tilde{\psi}_R(x)\tilde{\psi}_L(x) - \tilde{\psi}_R^\dagger(x)\tilde{\psi}_L(x) + \text{H.c.}],
\end{aligned}
\tag{13}
$$

where we have used $\tilde{\alpha}_\rho = \tilde{\psi}_\rho + \tilde{\psi}_\rho^\dagger$ and $\tilde{\beta}_\rho = (\tilde{\psi}_\rho - \tilde{\psi}_\rho^\dagger)/i$. While it gaps $\tilde{\alpha}_L$ and $\tilde{\beta}_R$, this Hamiltonian leaves the fields $\tilde{\alpha}_R, \tilde{\beta}_L$ gapless. Notice that strictly speaking, $\tilde{t}_a$ must be tuned to a multicritical point for the low-energy theory to remain identical. However, since we will soon break the self-duality of the problem, this will not be important.

The auxiliary model simplifies our analysis, as it allows us to formulate the problem in terms of the chiral bosonic modes η_R and η_L, such that $\tilde{\psi}_\rho = e^{i\eta_\rho}$. Mathematically, the Hamiltonian in Eq. (13) describes two edge modes of a $\nu = 1/m$ fractional quantum Hall state, coupled by a specific combination of ferromagnetic and superconducting terms.

Next, we include the physical coupling between the edge modes across the trench,

$$
\begin{aligned}
H_{\text{trench}} &= i\tilde{t}(\varphi) \int_0^l dx\, \tilde{\alpha}_R(x)\tilde{\beta}_L(x) \\
&= \tilde{t}(\varphi) \int_0^l dx[\tilde{\psi}_R(x)\tilde{\psi}_L(x) + \tilde{\psi}_R^\dagger(x)\tilde{\psi}_L(x) + \text{H.c.}],
\end{aligned}
$$

$$(14)$$

where $\varphi = 2\pi \frac{\Phi}{h/2e}$, and $\Phi = nh/2e$ is the flux through the center of the annulus. In the gauge in which the flux only enters into $\tilde{t}(\varphi)$, we have $\tilde{t}(\varphi) = \tilde{t}_0 \cos\left(\frac{\varphi}{2}\right)$.

Finally, it is necessary to introduce the correct boundary conditions, such that $\tilde{\alpha}_R \to \tilde{\beta}_L$ at $x = 0$ and $\tilde{\beta}_L \to \tilde{\alpha}_R$ at $x = l$ [see Fig. 3(c)]. This can be implemented by extending the model to $-\infty < x < \infty$ and strongly coupling α_R and β_L beyond the ends of the physical system, such that they acquire a large gap in these regions. Within the auxiliary model, formulated in terms of the two η fields, we can do this by introducing strong superconducting terms for $x < 0$ and $x > l$:

$$
H_{\text{bc}} = \Delta_{\text{bc}} \int_{x<0, x>l} dx[\tilde{\psi}_R(x)\tilde{\psi}_L(x) + \text{H.c.}]. \quad (15)
$$

The full auxiliary model is depicted in Fig. 3(d). Alternatively, note that one can also use a ferromagnetic term. This would not change our conclusions regarding the existence of zero modes.

While the choice of coupling constants $\tilde{t}_a$ and Δ_{bc} seems arbitrary, unphysical zero-energy degrees of freedom may appear if these are not properly chosen. In order to avoid these, we first choose the auxiliary coupling constant such that $\text{sgn}(\tilde{t}_a) = \text{sgn}(\Delta_{\text{bc}})$ (otherwise the coefficient of the term $i\tilde{\beta}_R\tilde{\alpha}_L$ changes sign at $x = 0, l$).

An additional consistency condition is obtained by noting that no physical zero-energy modes should appear in the absence of flux. This leads to the constraint $\text{sgn}(\Delta_{\text{bc}}) = \text{sgn}[\tilde{t}(\varphi = 0)]$.

To be consistent with these constraints, the coefficients of our auxiliary model must satisfy

$$
\text{sgn}(\tilde{t}_a) = \text{sgn}(\Delta_{\text{bc}}) = \text{sgn}(\tilde{t}_0). \quad (16)
$$

Clearly, the gap does not close as long as the various coupling constants do not change sign. In particular, the presence (or absence) of zero modes is not affected by varying the various parameters without altering their signs. We may therefore choose $\tilde{t}_0 = \tilde{t}_a |\cos\left(\frac{\varphi}{2}\right)|^{-1}$, in which case the Hamiltonian in the region $0 < x < l$ takes the form

$$
\begin{aligned}
&H_{\text{trench}} + H_{\text{auxiliary}} \\
&= \tilde{t}_a \int_0^l dx\Big\{\tilde{\psi}_R(x)\tilde{\psi}_L(x)\Big[1 + \text{sgn}\left(\cos\frac{\varphi}{2}\right)\Big] \\
&\quad - \tilde{\psi}_R^\dagger(x)\tilde{\psi}_L(x)\Big[1 - \text{sgn}\left(\cos\frac{\varphi}{2}\right)\Big] + \text{H.c.}\Big\}. \quad (17)
\end{aligned}
$$

While the trench allows us to continuously vary φ, we take the discrete values $\varphi = 2\pi n$, where n counts the number of $h/2e$ vortices. As Eq. (17) implies, if φ is an even multiple of 2π, the Hamiltonian reduces to superconducting terms

throughout space, thus preventing the existence of zero-energy modes [see Fig. 3(e)]. On the other hand, if φ is an odd multiple of 2π, it is clear that the superconductor in the region $0 < x < l$ is replaced by a ferromagnet and we end up with the S-F-S configuration studied in Refs. [17–19] [see Fig. 3(f)]. Notice that if we had chosen to implement the boundary conditions in Eq. (15) using ferromagnetic terms, we would end up with an F-S-F configuration for odd multiples of 2π and ferromagnetic terms throughout space for even multiple of 2π.

Following the results of Refs. [17–19], we conclude that the S-F-S and F-S-F configurations found above give rise to parafermion zero modes ξ_i, with $i = 1,2$, located at the interfaces $x = 0,l$. These operators satisfy

$$
\xi_1\xi_2 = \xi_2\xi_1 e^{i\frac{\pi}{m}}, \quad (18)
$$

and $\xi_i^{2m} = 1$. Equation (17) implies that the spectrum is 4π periodic as a function of φ.

We note that the interfaces correspond to the circular edges of the original annulus, so that this line of arguments indicates that $h/2e$ vortices in the FCSC system bind protected parafermionic zero modes. The parafermion nature of these excitations provides a natural generalization to the case where the bulk contains many vortices, each binding a zero mode generated by ξ_i ($i = 1 \cdots 2M$ is an arbitrary index labeling the zero modes). The parafermions generally satisfy the algebra

$$
\xi_i\xi_j = \xi_j\xi_i e^{i\frac{\pi}{m}\text{sgn}(i-j)}, \quad (19)
$$

from which one can infer a ground-state degeneracy of $(2m)^M$ for $2M$ vortices.

Once our annular system is transformed into the setup presented in Fig. 3(f) for an odd number of vortices, it is natural to ask whether we can control the relative phase between the two effective superconducting order parameters and measure the Josephson effect, which was previously shown to be $4\pi m$ periodic [18,19].

Recall that the superconductors shown in Fig. 3(f) were introduced to impose the boundary conditions and, in particular, do not correspond to the physical superconductor in proximity to our system. Nevertheless, we argue that such an effective Josephson junction can be generated by creating a physical Josephson junction in our system. This is done by considering a physical weak link cutting the physical s-wave superconductor at a fixed radial coordinate into two concentric annuli [see Fig. 1(b)]. This allows us to control the relative superconducting phases between the external and the internal parts of our system by connecting the two edges with an external superconducting wire, through which flux is inserted. Notice that coupling between electrons across the cut can effectively stitch the two parts of the system, leading to a gapped FCSC phase throughout the system (including the area above the cut).

Since the edges of our annular system correspond to the interfaces in the auxiliary configuration, we effectively control the relative phases between the two auxiliary superconductors shown in Fig. 3(f) [61]. Examining the quasi-one-dimensional regime, in which coupling between the two edge modes of our annular system is induced, the arguments above indicate that the junction shown in Fig. 1(b) gives rise to a $4\pi m$-periodic Josephson effect. Notice that the radial width of the

junction must be comparable to the correlation length in the bulk, allowing anyons to tunnel between the inner and the outer edges.

V. CONCLUSIONS

In this work, we have demonstrated that a FCSC phase can be stabilized in an array of coupled wires in the presence of Rashba SOC, Zeeman field, superconducting proximity effects, and strong interactions. The resulting phase was found to give rise to a parafermionic edge theory, whose central charge is $c = \frac{2m-1}{m+1}$, leading to a thermal conductance of the form $G_Q = \frac{\pi^2 k_B^2 T}{3h}(\frac{2m-1}{m+1})$. In this theory, the electron has an anomalous tunneling density of states of the form $N(\omega) \propto \omega^{m-1}$. We have additionally found that $h/2e$ vortices in such a system bind parafermionic zero modes, with quantum dimension $\sqrt{2m}$.

Clearly, the FCSC phase we construct is topologically ordered. While we leave the detailed study of the bulk excitations to future studies, we anticipate that the topologically distinct bulk excitations will be associated with the various low-energy sectors of the parafermionic edge theory through the bulk-edge correspondence. The low-energy sectors are generated by the primary fields of the parafermion CFT, which can be labeled by $\Phi_{[k,\bar{k}]}$ [16], where the integers k and $\bar{k}$ are defined mod $4m$, and $k + \bar{k}$ is even. In terms of these, the parafermion fields are given by $\psi_n = \Phi_{[2n,0]}$ and $\bar{\psi}_n = \Phi_{[0,2n]}$ (with $n = 1, \ldots, 2m - 1$), and the spin operators σ_n are given by $\sigma_n = \Phi_{[n,n]}$.

However, in identifying the deconfined bulk excitations with the primary fields of the edge CFT, we must exclude the operators which acquire a nontrivial phase as they wind around the electron, which in our case is identified with the field ψ_m (or $\bar{\psi}_m$). In particular, since the electron acquires a phase of π as it winds around a vortex, the corresponding field must be associated with a confined excitation (i.e., the energy of two such excitations diverges as we separate them [62]). More generally, the phase associated with winding $\Phi_{[k,\bar{k}]}$ around the electron ψ_m ($\bar{\psi}_m$) is given by $\gamma_{[k,\bar{k}]} = \pi k$ ($\bar{\gamma}_{[k,\bar{k}]} = \pi \bar{k}$) [16]. This shows, for example, that while the parafermion fields ψ_n are all deconfined in the bulk, the spin operators σ_n, with odd n, must be confined.

It has recently been shown that repulsive interactions can stabilize a time-reversal invariant topological superconducting (TRITOPS) phase in quantum wires [54–59]. It would be interesting to consider an array of such 1D systems as a possible realization of a fractional TRITOPS in 2D.

APPENDIX A: THE RENORMALIZATION-GROUP EQUATIONS OF THE SELF-DUAL SINE-GORDON MODEL

1. The ϵ expansion

The Hamiltonians describing either the inter- or intrawire coupling terms, discussed in the main text, can be written as

$$H = \int dx \left[\frac{1}{2\pi m}(\partial_x \eta_1)^2 + \frac{1}{2\pi m}(\partial_x \eta_2)^2 + \frac{\tilde{B}}{a^2} \cos(\eta_1 - \eta_2) + \frac{\tilde{\Delta}}{a^2} \cos(\eta_1 + \eta_2) \right],$$

where η_1 (η_2) is a right- (left-)moving mode satisfying

$$[\eta_j(x), \eta_j(x')] = m\pi i(-1)^j \text{sign}(x - x'),$$

and the units were chosen such that the Fermi velocity is $v = 1$. Specifically, in the main text, the coefficients were tuned to the self-dual line, such that $\tilde{B} = \tilde{\Delta}$.

To write the Hamiltonian in a more convenient form, we define

$$\varphi = \frac{\eta_1 - \eta_2}{2\sqrt{\pi m}},$$

$$\theta = \frac{\eta_1 + \eta_2}{2\sqrt{\pi m}}.$$

The commutation relations of these fields are given by

$$[\varphi(x), \theta(x')] = i\Theta(x - x').$$

In terms of these, the Hamiltonian takes the form

$$H = \int dx \left[(\partial_x \theta)^2 + (\partial_x \varphi)^2 + \frac{\tilde{B}}{a^2} \cos(2\sqrt{\pi m}\varphi) + \frac{\tilde{\Delta}}{a^2} \cos(2\sqrt{\pi m}\theta) \right].$$

We next wish to isolate the explicit cutoff dependence by writing the cosines in terms of their normal-ordered versions:

$$\cos(2\sqrt{\pi m}\varphi) =: \cos(2\sqrt{\pi m}\varphi) : e^{-2m\pi\langle\varphi^2\rangle},$$

$$\cos(2\sqrt{\pi m}\theta) =: \cos(2\sqrt{\pi m}\theta) : e^{-2m\pi\langle\theta^2\rangle},$$

where the averages are taken with respect to the quadratic part of the Hamiltonian.

Denoting the small distance cutoff by a and the large distance cutoff by L, we find that

$$e^{-2m\pi\langle\varphi^2\rangle} = e^{-2m\pi\langle\theta^2\rangle} = \left(\frac{a}{L}\right)^m.$$

Therefore, the Hamiltonian can be written in the form

$$H = \int dx \left[(\partial_x\theta)^2 + (\partial_x\varphi)^2 + \frac{\tilde{B}}{L^2}\left(\frac{a}{L}\right)^{m-2} : \cos(2\sqrt{\pi m}\varphi) : +\frac{\tilde{\Delta}}{L^2}\left(\frac{a}{L}\right)^{m-2} : \cos(2\sqrt{\pi m}\theta) : \right].$$

In performing the renormalization group, we quantify the dependence of the coefficients on $l = \ln\frac{L}{a}$.

At tree level, we simply use the explicit cutoff dependence of the coefficients to calculate $\frac{d\bar{B}}{dl}, \frac{d\bar{\Delta}}{dl}$, with $\bar{B} = \tilde{B}(\frac{a}{L})^{m-2}, \bar{\Delta} = \tilde{\Delta}(\frac{a}{L})^{m-2}$. The resulting tree-level RG equations are given by

$$\frac{d\bar{B}}{dl} = (2-m)\bar{B},$$

$$\frac{d\bar{\Delta}}{dl} = (2-m)\bar{\Delta},$$

giving a flow to weak coupling for $m > 2$. This is true in particular at the self-dual point $\tilde{B} = \tilde{\Delta} = \tilde{\lambda}$ that we wish to focus on.

Clearly, if a flow to large coupling is to occur for large λ, it must result from higher-order terms. The next possible nonvanishing correction to the RG equation of λ is of the order of λ^3, as the second-order correction vanishes at the self-dual line. Indeed, if the λ^3 term has a positive coefficient, it induces a flow to large couplings for large λ. However, for such a term to overcome the negative contribution of the first-order term, λ should be of the order of 1 (assuming the coefficients are of the order of 1 and recalling that in our model, $m = 3, 5$, etc.). Such a situation steps beyond the range of validity of the perturbative RG analysis.

To overcome the above technical difficulty, we study the situation in which m is slightly above its marginal value: $m = 2 + \epsilon$, with $\epsilon \ll 1$. In this case, the negative first-order contribution is proportional to ϵ,

$$\frac{d\bar{B}}{dl} = -\epsilon B,$$

$$\frac{d\bar{\Delta}}{dl} = -\epsilon\Delta,$$

and therefore if the third-order contribution is positive, the critical point between the two regimes is controlled by the small parameter ϵ and is therefore expected to be within the range of validity of the perturbative RG analysis. Indeed, we will find such a critical point satisfying $\lambda_c \propto \sqrt{\epsilon}$.

The critical point found for small ϵ indicates that a similar critical point exists for $\epsilon = 1$ as well, above which the coupling constants flow to large coupling (assuming no additional critical points are induced as ϵ is increased from $0 < \epsilon \ll 1$ to $\epsilon = 1$).

We next turn to explicitly derive the form of the third-order RG equations. The analysis presented below closely parallels the analysis presented in Ref. [47].

2. Third-order RG equations and the phase diagram

To calculate the higher orders of the renormalization-group equations, we generally write the partition function as

$$Z = \int D\varphi\, e^{-S_0 - S_1},$$

with

$$S_0 = \tfrac{1}{2}\int d\tau dx [(\partial_\tau\varphi)^2 + (\partial_x\varphi)^2],$$

$$S_1 = \int \frac{d\tau dx}{L^2} \{\bar{B} : \cos[\sqrt{8\pi(1+\delta_B)}\varphi] : +\bar{\Delta} : \cos[\sqrt{8\pi(1+\delta_\Delta)}\theta] : \},$$

where θ is related to φ according to the condition

$$i\partial_\mu\varphi = \epsilon^{\mu\nu}\partial_\nu\theta. \tag{A1}$$

In addition, we have defined $\bar{B} = \tilde{B}(\frac{a}{L})^{2\delta_B}, \bar{\Delta} = \tilde{\Delta}(\frac{a}{L})^{2\delta_\Delta}$.

In order to follow the strategy outlined above, we assume δ_B and δ_Δ are small. As these parameters flow as well, we will write the third-order RG equations for $\bar{B}, \bar{\Delta}, \delta_B, \delta_\Delta$. Once these are derived, we will focus on the self-dual line defined according to $\bar{B} = \bar{\Delta} = \bar{\lambda}$ and $\delta_B = \delta_\Delta = \frac{\epsilon}{2}$.

To derive the RG equations, we expand the partition function in orders of S_I,

$$Z = \int D\varphi D\theta e^{-S_0} \left(1 - S_I + \frac{1}{2}S_I^2 - \frac{1}{6}S_I^3 + \cdots \right). \tag{A2}$$

Next, we will use the operator product expansions (OPEs) of the resulting high orders to get corrections to the original action.

Taking only the first order into account, we get the contribution

$$\frac{d\bar{B}}{dl} = -2\delta_B \bar{B},$$

$$\frac{d\bar{\Delta}}{dl} = -2\delta_\Delta \bar{\Delta}.$$

To second order, terms of the form $\bar{B}^2$ and $\bar{\Delta}^2$ renormalize the kinetic term. Notice that we discard the nonsingular term of the order of $\bar{B}\bar{\Delta}$, which results in an irrelevant term.

We first calculate the $\bar{B}^2$ component of $S_2 = -\frac{1}{2}S_I^2$,

$$-\frac{\bar{B}^2}{2} \int d^2x_1 d^2x_2 L^{-4} : \cos[\sqrt{8\pi(1+\delta_B)}\varphi(\vec{x}_1)] :: \cos[\sqrt{8\pi(1+\delta_B)}\varphi(\vec{x}_2)] : . \tag{A3}$$

In order to calculate the OPE [47], we use the definition of normal ordering to write

$$: \cos[\sqrt{8\pi(1+\delta_B)}\varphi(\vec{x}_1)] :: \cos[\sqrt{8\pi(1+\delta_B)}\varphi(\vec{x}_2)] := e^{8\pi(1+\delta_B)\langle\varphi^2\rangle} \cos[\sqrt{8\pi(1+\delta_B)}\varphi(\vec{x}_1)] \cos[\sqrt{8\pi(1+\delta_B)}\varphi(\vec{x}_2)].$$

This can be rewritten as

$$\tfrac{1}{2}e^{8\pi(1+\delta_B)\langle\varphi^2\rangle}(\cos[\sqrt{8\pi(1+\delta_B)}\{\varphi(\vec{x}_1)+\varphi(\vec{x}_2)\}] + \cos[\sqrt{8\pi(1+\delta_B)}\{\varphi(\vec{x}_1)-\varphi(\vec{x}_2)\}]).$$

Writing the two cosines in terms of their normal-ordered versions, we get

$$\tfrac{1}{2}\{: \cos[\sqrt{8\pi(1+\delta_B)}\{\varphi(\vec{x}_1)+\varphi(\vec{x}_2)\}] : \frac{1}{c(\vec{x}_1 - \vec{x}_2)} + : \cos[\sqrt{8\pi(1+\delta_B)}\{\varphi(\vec{x}_1)-\varphi(\vec{x}_2)\}] : c(\vec{x}_1 - \vec{x}_2)\},$$

with

$$c(\vec{x}_1 - \vec{x}_2) = e^{8\pi(1+\delta_B)\langle\varphi(\vec{x}_1)\varphi(\vec{x}_2)\rangle} = \left(\frac{|\vec{x}_1 - \vec{x}_2|}{L} \right)^{-4(1+\delta_B)}.$$

The first term results in irrelevant terms and is therefore ignored. The second term is dominated by the region in which the two points $\vec{x}_1$ and $\vec{x}_2$ are close to each other. This allows us to approximate

$$\cos[\sqrt{8\pi(1+\delta_B)}\{\varphi(\vec{x}_1)-\varphi(\vec{x}_2)\}] \approx 1 - 4\pi(1+\delta_B)[\varphi(\vec{x}_1)-\varphi(\vec{x}_2)]^2 = 1 - 4\pi(1+\delta_B)[(\vec{x}_1 - \vec{x}_2) \cdot \nabla\varphi(\vec{x})]^2,$$

where $\vec{x}$ is the center-of-mass coordinate. Plugging this back into Eq. (A3) and performing the integral over the relative coordinate $\vec{x}_1 - \vec{x}_2$, we get a correction of the form

$$2\pi^2 \ln\frac{L}{a} \bar{B}^2(1+\delta_B)\left\{ \frac{1}{2} \int [(\partial_x\varphi)^2 + (\partial_\tau\varphi)^2]d^2x \right\}.$$

Similarly, the $\bar{\Delta}^2$ terms give us (up to a constant)

$$: \cos[\sqrt{8\pi(1+\delta_\Delta)}\theta(\vec{x}_1)] :: \cos[\sqrt{8\pi(1+\delta_\Delta)}\theta(\vec{x}_2)] := -\frac{\pi(1+\delta_\Delta)|\vec{x}_1 - \vec{x}_2|^2}{\left(\frac{|\vec{x}_1 - \vec{x}_2|}{L}\right)^{4(1+\delta_\Delta)}} \{[\partial_x\theta(\vec{x})]^2 + [\partial_\tau\theta(\vec{x})]^2\}. \tag{A4}$$

Using Eq. (A1) and integrating over the relative coordinate, we obtain the correction

$$-2\pi^2 \ln\frac{L}{a} \bar{\Delta}^2(1+\delta_\Delta)\left\{ \frac{1}{2} \int [(\partial_x\varphi)^2 + (\partial_\tau\varphi)^2]d^2x \right\}.$$

Taken together, the second-order corrections are given by

$$S_2 = 2\pi^2 \ln\frac{L}{a}\{\bar{B}^2(1+\delta_B) - \bar{\Delta}^2(1+\delta_\Delta)\}\left\{ \frac{1}{2} \int [(\partial_x\varphi)^2 + (\partial_\tau\varphi)^2]d^2x \right\}.$$

The second-order term clearly renormalizes the kinetic part of the action.

The third-order contributions are given by a combination of $S_3^a = \frac{1}{6}S_I^3$ and $S_3^b = S_1 S_2$ [the latter contribution arises when one reexponentiates the partition function in Eq. (A2)].

We first look at the S_3^a term. The corrections of the type $\bar{B}^3$ and $\bar{B}\bar{\Delta}^2$ renormalize the B term, while terms of the form $\bar{\Delta}^3$ and $\bar{\Delta}\bar{B}^2$ renormalize the Δ term. Let us first look at the $\bar{B}^3$-order term:

$$\frac{1}{6}\bar{B}^3 \int \Pi_{n=1}^3 \left\{ \frac{d^2 x_n}{L^2} : \cos[\sqrt{8\pi(1+\delta_B)}\varphi(\vec{x}_n)] : \right\}.$$

Using the OPE and dropping the nonsingular term, we get the correction [47]

$$\frac{\bar{B}^3}{8L^6} \int d^2 x_1 d^2 x_2 d^2 x_3 \left(\frac{L^2|\vec{x}_1 - \vec{x}_2|^2}{|\vec{x}_1 - \vec{x}_3|^2|\vec{x}_2 - \vec{x}_3|^2} \right)^m : \cos\{\sqrt{8\pi(1+\delta_B)}[\varphi(\vec{x}_1) + \varphi(\vec{x}_2) - \varphi(\vec{x}_3)]\} : .$$

Clearly, the most dominant contributions arise when two coordinates approach each other: either $\vec{x}_1 \to \vec{x}_3$ or $\vec{x}_2 \to \vec{x}_3$. However, these divergences are disconnected and are therefore discarded. Thus, the only singular contribution arises when the three different coordinates approach each other. Taking this into account, we approximate

$$: \cos\{\sqrt{8\pi(1+\delta_B)}[\varphi(\vec{x}_1) + \varphi(\vec{x}_2) - \varphi(\vec{x}_3)]\} :\approx: \cos[\sqrt{8\pi(1+\delta_B)}\varphi(\vec{x})] : ,$$

where $\vec{x}$ is the center-of-mass coordinate and therefore

$$\frac{1}{8L^6} \int d^2 x_1 d^2 x_2 d^2 x_3 \left(\frac{L^2|\vec{x}_1 - \vec{x}_2|^2}{|\vec{x}_1 - \vec{x}_3|^2|\vec{x}_2 - \vec{x}_3|^2} \right)^2 : \cos[\sqrt{8\pi(1+\delta_B)}\varphi(\vec{x})] : .$$

Integrating over the relative coordinates and subtracting disconnected terms, we find the correction [47]

$$\frac{2\pi^2 \bar{B}^3}{L^2} \left[\ln\left(\frac{L}{a}\right) \right]^2 \int d^2 x : \cos[\sqrt{8\pi(1+\delta_B)}\varphi(\vec{x})] : .$$

Similar considerations show that the $\bar{B}\bar{\Delta}^2$ term provides a contribution of the form

$$\frac{\pi^2 \bar{B}\bar{\Delta}^2}{L^2} \left\{ \ln\left(\frac{L}{a}\right) - 2\left[\ln\left(\frac{L}{a}\right) \right]^2 \right\} \int d^2 x : \cos[\sqrt{8\pi(1+\delta_B)}\varphi(\vec{x})] : .$$

The remaining contribution is of the form S_3^b. The contribution to the B term is given by

$$2\pi^2 \ln\frac{L}{a} \bar{B}\{\bar{B}^2(1+\delta_B) - \bar{\Delta}^2(1+\delta_\Delta)\} \left\{ \frac{1}{2} \int d^2 x_1 d^2 x_2 \mu^2 \{[\partial_x \varphi(\vec{x}_1)]^2 + [\partial_\tau \varphi(\vec{x}_1)]^2\} : \cos[\sqrt{8\pi(1+\delta_B)}\varphi(\vec{x}_2)] : \right\}.$$

Keeping only the third orders in the various scaling parameters and using the corresponding OPE, we get

$$-2\pi^2 \left(\ln\frac{L}{a} \right)^2 \bar{B}\{\bar{B}^2 - \bar{\Delta}^2\} \int d^2 x : \cos\{\sqrt{8\pi(1+\delta_B)}[\varphi(\vec{x})]\} : .$$

Analogous corrections can be derived for the Δ field.

Summing the above corrections, we find that the renormalized action is given by

$$S = S_I + 2\pi^2 \ln\frac{L}{a}\{\bar{B}^2(1+\delta_B) - \bar{\Delta}^2(1+\delta_\Delta)\}\left\{ \frac{1}{2} \int [(\partial_x \varphi)^2 + (\partial_\tau \varphi)^2] d^2 x \right\}$$

$$+ \frac{\pi^2 \bar{B}\bar{\Delta}^2}{L^2} \ln\left(\frac{L}{a}\right) \int d^2 x : \cos[\sqrt{8\pi(1+\delta_B)}\varphi(\vec{x})] :$$

$$+ \frac{\pi^2 \bar{\Delta}\bar{B}^2}{L^2} \ln\left(\frac{L}{a}\right) \int d^2 x : \cos[\sqrt{8\pi(1+\delta_\Delta)}\theta(\vec{x})] : .$$

Based on the above, the RG equations for the coefficients of the cosine terms are given by

$$\frac{d\bar{B}}{dl} = -2\delta_B \bar{B} + \pi^2 \bar{B}\bar{\Delta}^2,$$

$$\frac{d\bar{\Delta}}{dl} = -2\delta_\Delta \bar{\Delta} + \pi^2 \bar{\Delta}\bar{B}^2.$$

The correction to the kinetic term can be eliminated by rescaling the φ and θ fields. This induces a change in the variables δ_B, δ_Δ, leading to the RG equations:

$$\frac{d\delta_B}{dl} = -2\pi^2(1+\delta_B)[\bar{B}^2(1+\delta_B) - \bar{\Delta}^2(1+\delta_\Delta)],$$

$$\frac{d\delta_\Delta}{dl} = -2\pi^2(1+\delta_\Delta)[\bar{\Delta}^2(1+\delta_\Delta) - \bar{B}^2(1+\delta_B)].$$
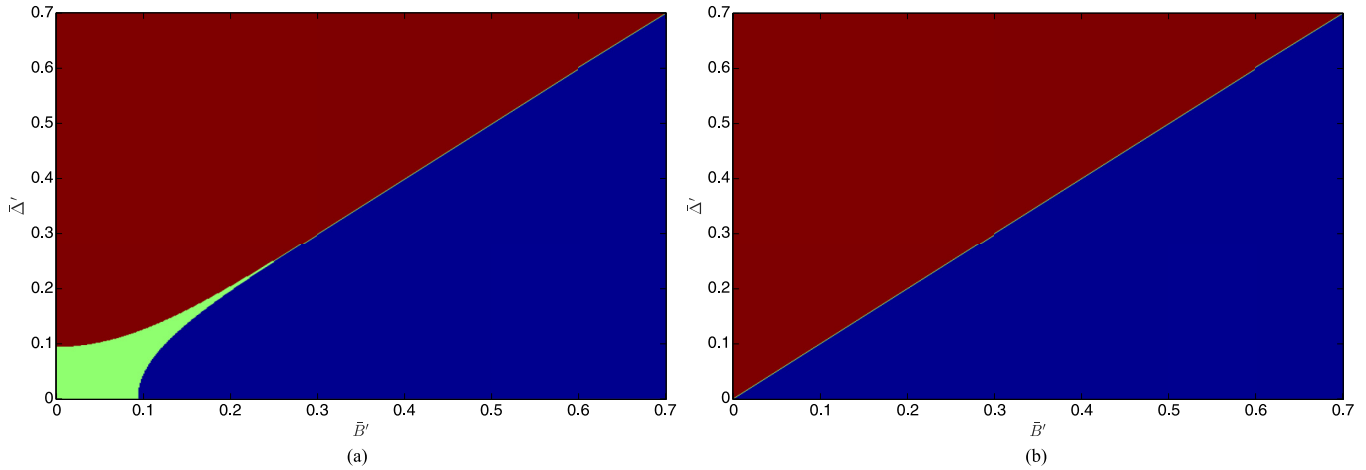
FIG. 4. The phase diagrams for (a) $\epsilon = 0.2$ and (b) $\epsilon = -0.2$. The red region corresponds to a Δ-dominated phase, the blue region corresponds to a B-terms phase, and the green regions correspond to gapless states.

Rescaling $\bar{B}' = \pi^2 \bar{B}, \bar{\Delta}' = \pi^2 \bar{\Delta}$, we finally write the RG equations,

$$\frac{d\bar{B}'}{dl} = -2\delta_B \bar{B}' + \bar{B}'\bar{\Delta}'^2,$$

$$\frac{d\bar{\Delta}}{dl} = -2\delta_\Delta \bar{\Delta}' + \bar{\Delta}'\bar{B}'^2,$$

$$\frac{d\delta_B}{dl} = -2(1 + \delta_B)[\bar{B}'^2(1 + \delta_B) - \bar{\Delta}'^2(1 + \delta_\Delta)],$$

$$\frac{d\delta_\Delta}{dl} = -2(1 + \delta_\Delta)[\bar{\Delta}'^2(1 + \delta_\Delta) - \bar{B}'^2(1 + \delta_B)]. \tag{A5}$$

Figure 4 presents the phase diagram resulting from the solution of the RG equations shown in Eq. (A5). Specifically, the different colors represent different phases based on the flow equations: The red regions represent a Δ-dominated phase, the blue region represents a B-dominated phase, and the green regions represent a gapless state. Figure 4(a) [4(b)] was generated by studying the properties of the RG equations for various initial values of $\bar{B}', \bar{\Delta}'$ and $\delta_B = \delta_\Delta = \frac{\epsilon}{2}$, with $\epsilon = 0.2$ [$\epsilon = -0.2$].

3. Studying the self-dual line

Focusing on the self-dual line $\bar{B}' = \bar{\Delta}' = \bar{\lambda}$, $\delta_B = \delta_\Delta = \epsilon/2$, we get a single RG equation,

$$\frac{d\bar{\lambda}}{dl} = -\epsilon\bar{\lambda} + \bar{\lambda}^3,$$

accompanied by $\frac{d\epsilon}{dl} = 0$. We immediately find a multicritical point at $\bar{\lambda} = \sqrt{\epsilon}$, above which a flow to large $\bar{\lambda}$ ensues. This shows that if the coupling constants in the self-dual theory studied in the main text are large enough, the cosine terms flow to large coupling.

As we argued in the main text, if $\bar{\lambda}$ is tuned to the multicritical point, the low-energy field theory is not given by the original Luttinger-liquid fixed point, but rather by a parafermion CFT.

APPENDIX B: THE SCALING DIMENSION OF THE LOCAL ELECTRON FIELDS

In this section, we demonstrate that the scaling dimension of the local electron fields $\tilde{\alpha}_{nR}(x), \tilde{\beta}_{nL}(x)$ remains $m/2$ in the presence of the intrawire interacting term, which is taken to the critical point $\tilde{\Delta} = \tilde{B} = \lambda$:

$$\tilde{H}_\Delta + \tilde{H}_B = \lambda i \int dx \tilde{\beta}_{nR} \tilde{\alpha}_{nL}. \tag{B1}$$

We first note that since $\tilde{\alpha}_{nR}(x)$ and $\tilde{\beta}_{nL}(x)$ commute with the above interacting Hamiltonian, they remain right- and left-moving fields, respectively. To demonstrate this, we write the equations of motion of $\tilde{\alpha}_{nR}(x)$,

$$\frac{\partial}{\partial \tau} \tilde{\alpha}_{nR}(x,\tau) = [H, \tilde{\alpha}_{nR}(x,\tau)].$$

The Hamiltonian is composed of the kinetic chiral Luttinger-liquid Hamiltonian and the interacting Hamiltonian written in Eq. (B1). Since $\tilde{\alpha}_{nR}(x)$ commutes with the latter, we only need to calculate the commutation with the kinetic part,

$$H_K = \frac{v}{4\pi m} \lim_{\epsilon \to 0} \int \{\partial \eta_{nR}(x)\}\{\partial \eta_{nR}(x + \epsilon)\},$$

where we have used point splitting regularization. Since, by definition, $\tilde{\alpha}_{nR}(x) = e^{i\eta_{nR}} + e^{-i\eta_{nR}}$, we calculate the commutation relation with each vertex operator separately,

$$[H, e^{\pm i\eta_{nR}(x)}] = \frac{v}{4\pi m} \lim_{\epsilon \to 0} \int dx' [\{\partial \eta_{nR}(x')\}\{\partial \eta_{nR}(x' + \epsilon)\}e^{\pm i\eta_{nR}(x)} - e^{\pm i\eta_{nR}(x)}\{\partial \eta_{nR}(x')\}\{\partial \eta_{nR}(x' + \epsilon)\}]$$

$$= e^{\pm i\eta_{nR}(x)} \frac{v}{4\pi m} \lim_{\epsilon \to 0} \int dx' [e^{\mp i\eta_{n,R}} \{\partial \eta_{nR}(x')\}\{\partial \eta_{nR}(x' + \epsilon)\}e^{\pm i\eta_{nR}(x)} - \{\partial \eta_{nR}(x')\}\{\partial \eta_{nR}(x' + \epsilon)\}].$$

Using the commutation relations

$$[\eta_{nR}(x), \partial \eta_{nR}(x')] = -2\pi i m \delta(x - x')$$

and the Baker-Campbell-Hausdorff formula, we write

$$e^{\mp i\eta_{n,R}} \{\partial \eta_{nR}(x')\}e^{\pm i\eta_{nR}(x)} = \partial \eta_{nR}(x') \mp i[\eta_{nR}(x), \partial \eta_{nR}(x')] = \partial \eta_{nR}(x') \mp 2\pi m \delta(x - x'),$$

and therefore

$$[H, e^{\pm i\eta_{nR}(x)}] = \mp v e^{\pm i\eta_{nR}(x)} \partial \eta_{nR}(x) = -iv \partial e^{\pm i\eta_{nR}(x)}.$$

This gives us the equation of motion

$$\frac{\partial}{\partial \tau} \tilde{\alpha}_{nR}(x, \tau) = -iv \frac{\partial}{\partial x} \tilde{\alpha}_{nR}(x, \tau).$$

Defining $z = x + iv\tau$, we may write the above as

$$\frac{\partial}{\partial \bar{z}} \tilde{\alpha}_{nR}(x, \tau) = 0.$$

This shows that $\tilde{\alpha}_{nR}(z)$ remains a right mover in the presence of the interacting Hamiltonian (B1). Similarly, $\tilde{\beta}_{nL}$ satisfies $\frac{\partial}{\partial z} \tilde{\beta}_{nL}(x, \tau) = 0$ and is therefore a left mover. We note that the above analysis cannot be repeated for the fields $\tilde{\alpha}_{nL}$ and $\tilde{\beta}_{nR}$, which do not commute with the interacting Hamiltonian and are therefore not chiral.

Using the above result, we now turn to calculate the propagator of the remaining chiral fields and show that all corrections to the $\lambda = 0$ limit vanish identically. For example, calculating the propagator $g(z - z') = \langle \tilde{\alpha}_{nR}(z)\tilde{\alpha}_{nR}(z')\rangle$ and treating the interacting Hamiltonian shown in Eq. (B1) perturbatively, we can write the correction to any order p as

$$\delta g_p(z - z') \propto (\lambda i)^p \left\langle \tilde{\alpha}_{nR}(z)\tilde{\alpha}_{nR}(z')\Pi_{i=1}^{p} \int d^2 z_i \tilde{\beta}_{nR}(z_i, \bar{z}_i)\tilde{\alpha}_{nL}(z_i, \bar{z}_i)\right\rangle_0. \tag{B2}$$

Since the expectation value is done with respect to the kinetic Hamiltonian, we can treat $\tilde{\alpha}_{nL}$ as a function of $\bar{z}$ only and $\tilde{\beta}_{nR}$ as a function of z. Furthermore, we can use the symmetries of the kinetic Hamiltonian: First, we know that under rotations $z \to ze^{i\theta}, \bar{z} \to \bar{z}e^{-i\theta}$, the fields transform as $\tilde{\alpha}_{nR}(z) \to \tilde{\alpha}_{nR}(z)e^{-i\theta m/2}, \tilde{\alpha}_{nL}(\bar{z}) \to \tilde{\alpha}_{nL}(\bar{z})e^{i\theta m/2}$ (and the same relations for the β fields). This leads to the condition

$$\delta g_p[(z - z')e^{i\theta}] = e^{-i\theta m} \delta g_p[z - z'],$$

which is satisfied if $\delta g_p \propto (z - z')^{-m}$.

Under scale transformations, given by $z \to zd, \bar{z} \to \bar{z}d$, the fields transform as $\tilde{\alpha}_{nR}(z) \to \tilde{\alpha}_{nR}(z)d^{-m/2}, \tilde{\alpha}_{nL}(\bar{z}) \to \tilde{\alpha}_{nL}(\bar{z})d^{-m/2}$ (and similarly for the $\tilde{\beta}$ fields). In this case, we get the condition $\delta g_p[(z - z')d] = d^{-m+p(2-m)}\delta g_p[z - z']$, which is satisfied if $\delta g_p \propto (z - z')^{-m+p(2-m)}$. Clearly, we have reached a contradiction, which can only be solved if $\delta g_p[z - z'] = 0$ for any $p > 0$. This shows that all corrections to the propagator calculated in the absence of the interacting term vanish and the scaling dimension of $\tilde{\alpha}_{nR}$ and $\tilde{\beta}_{nL}$ therefore remains $m/2$.

We note that as the fields $\tilde{\beta}_{nR}$ and $\tilde{\alpha}_{nL}$ are no longer chiral, the full propagator is not a holomorphic (or antiholomorphic) function and the entire argument fails, as expected.

[1] A. P. Schnyder, S. Ryu, A. Furusaki, and A. W. W. Ludwig, Phys. Rev. B **78**, 195125 (2008).

[2] A. Kitaev, AIP Conf. Proc. **1134**, 22 (2009).

[3] L. Fu, Phys. Rev. Lett. **106**, 106802 (2011).

[4] T. H. Hsieh, H. Lin, J. Liu, W. Duan, A. Bansil, and L. Fu, Nat. Commun. **3**, 982 (2012).

[5] Y. Tanaka, Z. Ren, T. Sato, K. Nakayama, S. Souma, T. Takahashi, K. Segawa, and Y. Ando, Nat. Phys. **8**, 800 (2012).

[6] P. Dziawa, B. Kowalski, K. Dybko, R. Buczko, A. Szczerbakow, M. Szot, E. Łusakowska, T. Balasubramanian, B. M. Wojek, M. Berntsen *et al.*, Nat. Mater. **11**, 1023 (2012).

[7] S.-Y. Xu, C. Liu, N. Alidoust, M. Neupane, D. Qian, I. Belopolski, J. Denlinger, Y. Wang, H. Lin, L. Wray *et al.*, Nat. Commun. **3**, 1192 (2012).

[8] R.-J. Slager, A. Mesaros, V. Juričić, and J. Zaanen, Nat. Phys. **9**, 98 (2012).

[9] J. Kruthoff, J. de Boer, J. van Wezel, C. L. Kane, and R.-J. Slager, arXiv:1612.02007.

[10] C.-X. Liu, R.-X. Zhang, and B. K. VanLeeuwen, Phys. Rev. B **90**, 085304 (2014).

[11] C. Fang and L. Fu, Phys. Rev. B **91**, 161105 (2015).

[12] K. Shiozaki, M. Sato, and K. Gomi, Phys. Rev. B **91**, 155120 (2015).

[13] Z. Wang, A. Alexandradinata, R. J. Cava, and B. A. Bernevig, Nature (London) **532**, 189 (2016).

[14] N. Read and E. Rezayi, Phys. Rev. B **59**, 8084 (1999).

[15] I. Seroussi, E. Berg, and Y. Oreg, Phys. Rev. B **89**, 104523 (2014).

[16] A. B. Zamolodchikov and V. A. Fateev, Zh. Eksp. Teor. Fiz. **89**, 380 (1985).

[17] N. H. Lindner, E. Berg, G. Refael, and A. Stern, Phys. Rev. X **2**, 041002 (2012).

[18] D. J. Clarke, J. Alicea, and K. Shtengel, Nat. Commun. **4**, 1348 (2013).

[19] M. Cheng, Phys. Rev. B **86**, 195126 (2012).

[20] C. L. Kane, R. Mukhopadhyay, and T. C. Lubensky, Phys. Rev. Lett. **88**, 036401 (2002).

[21] J. C. Y. Teo and C. L. Kane, Phys. Rev. B **89**, 085101 (2014).

[22] J. Klinovaja and D. Loss, Phys. Rev. Lett. **111**, 196401 (2013).

[23] T. Neupert, C. Chamon, C. Mudry, and R. Thomale, Phys. Rev. B **90**, 205101 (2014).

[24] E. Sagi and Y. Oreg, Phys. Rev. B **90**, 201102 (2014).

[25] J. Klinovaja and Y. Tserkovnyak, Phys. Rev. B **90**, 115426 (2014).

[26] T. Meng and E. Sela, Phys. Rev. B **90**, 235425 (2014).

[27] R. A. Santos, C.-W. Huang, Y. Gefen, and D. B. Gutman, Phys. Rev. B **91**, 205141 (2015).

[28] E. Sagi, Y. Oreg, A. Stern, and B. I. Halperin, Phys. Rev. B **91**, 245144 (2015).

[29] G. Gorohovsky, R. G. Pereira, and E. Sela, Phys. Rev. B **91**, 245139 (2015).

[30] T. Meng, T. Neupert, M. Greiter, and R. Thomale, Phys. Rev. B **91**, 241106 (2015).

[31] D. F. Mross, A. Essin, and J. Alicea, Phys. Rev. X **5**, 011011 (2015).

[32] T. Meng, Phys. Rev. B **92**, 115152 (2015).

[33] E. Sagi and Y. Oreg, Phys. Rev. B **92**, 195137 (2015).

[34] T. Meng, A. G. Grushin, K. Shtengel, and J. H. Bardarson, Phys. Rev. B **94**, 155136 (2016).

[35] H. Isobe and L. Fu, Phys. Rev. B **92**, 081304 (2015).

[36] S. Sahoo, Z. Zhang, and J. C. Y. Teo, Phys. Rev. B **94**, 165142 (2016).

[37] T. Iadecola, T. Neupert, C. Chamon, and C. Mudry, Phys. Rev. B **93**, 195136 (2016).

[38] Y. Fuji, Y.-C. He, S. Bhattacharjee, and F. Pollmann, Phys. Rev. B **93**, 195143 (2016).

[39] P.-H. Huang, J.-H. Chen, P. R. S. Gomes, T. Neupert, C. Chamon, and C. Mudry, Phys. Rev. B **93**, 205123 (2016).

[40] A. Vaezi, Phys. Rev. B **87**, 035132 (2013).

[41] R. S. K. Mong, D. J. Clarke, J. Alicea, N. H. Lindner, P. Fendley, C. Nayak, Y. Oreg, A. Stern, E. Berg, K. Shtengel, and M. P. A. Fisher, Phys. Rev. X **4**, 011036 (2014).

[42] A. Vaezi, Phys. Rev. X **4**, 031009 (2014).

[43] R. M. Lutchyn, J. D. Sau, and S. Das Sarma, Phys. Rev. Lett. **105**, 077001 (2010).

[44] Y. Oreg, G. Refael, and F. von Oppen, Phys. Rev. Lett. **105**, 177002 (2010).

[45] J. D. Sau, R. M. Lutchyn, S. Tewari, and S. Das Sarma, Phys. Rev. Lett. **104**, 040502 (2010).

[46] J. Alicea, Phys. Rev. B **81**, 125318 (2010).

[47] D. Boyanovsky, J. Phys. A: Math. Gen. **22**, 2601 (1989).

[48] E. Domany and E. K. Riedel, Phys. Rev. B **19**, 5817 (1979).

[49] F. C. Alcaraz and R. Koberle, J. Phys. A **13**, L153 (1980).

[50] P. Dorey, R. Tateo, and K. E. Thompson, Nucl. Phys. B **470**, 317 (1996).

[51] P. B. Wiegmann, J. Phys. C: Solid State Phys. **11**, 1583 (1978).

[52] P. Lecheminant, A. O. Gogolin, and A. A. Nersesyan, Nucl. Phys. B **639**, 502 (2002).

[53] N. Read and D. Green, Phys. Rev. B **61**, 10267 (2000).

[54] E. Gaidamauskas, J. Paaske, and K. Flensberg, Phys. Rev. Lett. **112**, 126402 (2014).

[55] A. Haim, A. Keselman, E. Berg, and Y. Oreg, Phys. Rev. B **89**, 220504 (2014).

[56] J. Klinovaja and D. Loss, Phys. Rev. Lett. **112**, 246403 (2014).

[57] J. Klinovaja and D. Loss, Phys. Rev. B **90**, 045118 (2014).

[58] J. Danon and K. Flensberg, Phys. Rev. B **91**, 165425 (2015).

[59] A. Haim, K. Wölms, E. Berg, Y. Oreg, and K. Flensberg, Phys. Rev. B **94**, 115124 (2016).

[60] We note that depending on the specific details of the model, the role of even and odd number of vortices may interchange.

[61] Notice that the phase differences in the effective and the physical Josephson junctions play a similar role in changing the wave function of the low-energy electron operators. This indicates that changing the phase difference in the physical junction results in a phase difference in the effective junction as well.

[62] Notice that such confined excitation can be introduced to the system externally. For example, a vortex in a $p_x + i p_y$ superfluid is confined, but it can be induced by applying an external effective magnetic field.